COMPUTATIONAL METHODS IN ENERGY TECHNOLOGY

Assignment No. 01

1D STEADY CONDUCTION HEAT TRANSFER CASE IN CYLINDRICAL WALLS

Submitted by: Rajnesh Kumar

Date of Submission: 02-Oct-2024

Submitted to: Prof. Carlos David Perez Segarra

Table of Contents

PROBLEM DESCRIPTION

A cylinder as shown in Fig. 1 has inner radius R_A, external radius R_B and height H. The cylinder is surrounded by fluids at its inner and outer boundaries. The heat transfer coefficient and temperature of inner fluids are α_A and T_A, while that of external are α_B and T_B. The cylinder is made up material with thermal conductivity $\boldsymbol{\lambda}$ and there is volumetric heat generation q_v inside the cylinder. The values of these parameters can be found in Table 1.

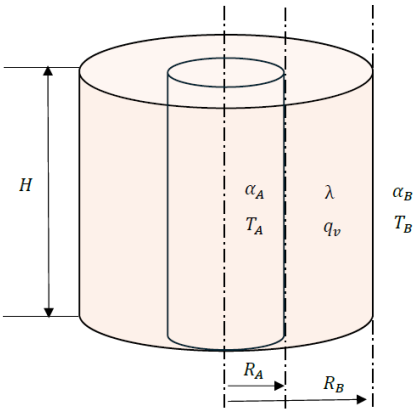

Fig. 1: The cylinder case

Table 1: Physical and Numerical data

Physical data	
R_A	0.5 [m]
R_B	0.25 [m]
H	1 [m]
T_A	80 [C]
T_B	40 [C]
α_A	30 [W/m^{2}K]
α_B	10 [W/m^{2}K]
$\boldsymbol{\lambda}$	15 [W/m.K]
q_v	2000 [W/m^2]
Numerical data	
N	100
Tolerance	10^{-12}
Max Iterations	10^8

ANALYTICAL SOLUTION

Given constant thermal conductivity and volumetric heat generation, and with adiabatic top and bottom surfaces, the problem reduces to a one-dimensional heat conduction problem, where temperature and heat transfer vary only with the radial coordinate as shown in Fig. 2.

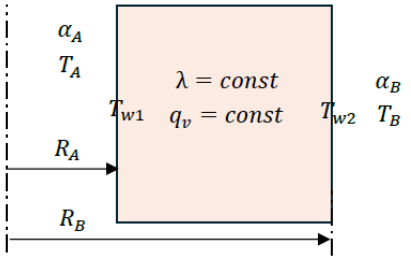

Fig. 2: Problem reduction to 1D

From formula 3.2, the analytical solution for 1D steady heat conduction in cylinder is as given as:

$$T = -\frac{q_v}{4\lambda}r^2 + C_1 \ln(r) + C_2 \longrightarrow (1)$$

$$\dot{q_r} = \frac{1}{2}q_v r - \lambda\frac{C_1}{r} \longrightarrow (2)$$

- Boundary Conditions

To get the values of constants C_1 and C_2, the boundary conditions are applied.

At $r = R_A \longrightarrow T(r) = T_{w1}$

At $r = R_B \longrightarrow T(r) = T_{w2}$

After putting these in eq. (1), and simplifying we get the following equations.

$$C_1 \ln(R_A) + C_2 - T_{w1} + 0T_{w2} = \frac{q_v}{4\lambda}{R_A}^2 \longrightarrow (i)$$

$$C_1 \ln(R_B) + C_2 + 0T_{w1} - T_{w2} = \frac{q_v}{4\lambda}{R_B}^2 \longrightarrow (ii)$$

However, there are four unknowns, and we only have two equations. Hence, by applying the energy balance on each wall we have.

For left wall

$$q_{conv} = q_r(R_A)$$

$$\alpha_A(T_A - T_{w1}) = \frac{1}{2}q_v R_A - \lambda\frac{C_1}{R_A}$$

$$\frac{\lambda}{R_A}C_1 + 0C_2 - \alpha_A T_{w1} + 0T_{w2} = \frac{1}{2}q_v R_A - \alpha_A T_A \longrightarrow (iii)$$

For right wall

$$q_r(R_B) = q_{conv}$$

$$\frac{1}{2}q_v R_B - \lambda\frac{C_1}{R_B} = \alpha_B(T_{w2} - T_B)$$

$$\frac{\lambda}{R_B}C_1 + 0C_2 - 0T_{w1} + \alpha_B T_{w2} = \frac{1}{2}q_v R_B + \alpha_B T_B \longrightarrow (iv)$$

Now we have a set of 4 equations and 4 unknowns. In matrix form these equations can be written as

$$\begin{bmatrix} \ln(R_A) & 1 & -1 & 0 \\ \ln(R_B) & 1 & 0 & -1 \\ \frac{\lambda}{R_A} & 0 & \alpha_A & 0 \\ \frac{\lambda}{R_B} & 0 & 1 & \alpha_B \end{bmatrix} \begin{bmatrix} C_1 \\ C_2 \\ T_{w1} \\ T_{w2} \end{bmatrix} = \begin{bmatrix} \frac{q_v}{4\lambda} {R_A}^2 \\ \frac{q_v}{4\lambda} {R_B}^2 \\ \frac{1}{2} q_v R_A - \alpha_A T_A \\ \frac{1}{2} q_v R_B + \alpha_B T_B \end{bmatrix}$$

The values of C_1, and C_2 can be obtained by solving the matrix. Afterwards these values are substituted in the equation (1) to get the temperature profile.

NUMERICAL SOLUTION

Domain Discretization

To solve the problem numerically, the first step is to discretize the domain. As shown in Fig. 3, the domain has been divided into N control volumes with uniform mesh spacing and a node is placed at the center of control volume. There are also nodes at the boundaries. Therefore, we have N+2 nodes.

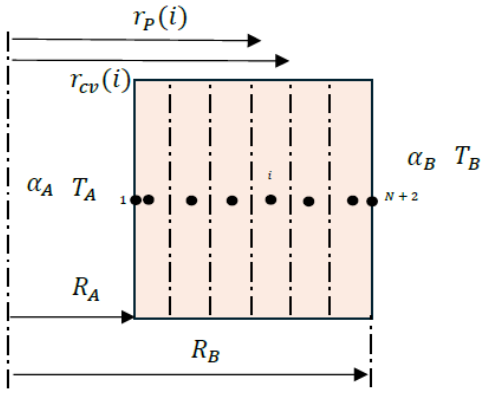

Fig. 3: Domain discretization

- Mesh and Nodal Positions

Since the mesh spacing is uniform, the position of control volumes can be given as:

$$r_{cv}(i) = R_A + (i-1)\Delta r \; for \; i = 1 \; to \; N+1$$

$$where \; \Delta r = \frac{R_B - R_A}{N}$$

And the position of the nodes is given as:

$$r_P(1) = R_A$$

$$r_P(i) = \frac{[r_{cv}(i) - r_{cv}(i-1)]}{2} \; for \; i = 2 \; to \; N+1$$

$$r_P(N+2) = R_B$$

- Areas and Volumes

For control volumes, the areas of east, west face and volumes are defined as:

$$S_e(i) = 2\pi r_{cv}(i)H$$

$$S_w(i) = 2\pi r_{cv}(i-1)H$$

$$V_p(i) = \pi[r_{cv}(i)^2 - r_{cv}(i-1)^2]H$$

Discretization of Equations

- Internal Nodes (i = 1 to N+1)

Energy balance is applied at general node P on the rod, as shown in Fig. 4. Since there is no transient term, the energy balance for the node P can be written as:

$$Q_w - Q_e + Q_{vp} = 0$$

$$-\lambda_w \frac{dT}{dr}|_w S_w + \lambda_e \frac{dT}{dx}|_e S_e + q_v V_p = 0$$

$$-\lambda_w \frac{T_p - T_w}{d_{PW}} + \lambda_e \frac{T_e - T_p}{d_{PE}} + q_v V_p = 0$$

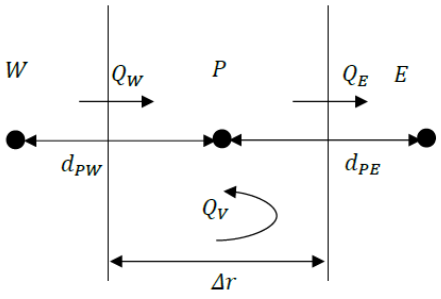

Fig. 4: General node P

The general form of discretized equation for Gauss-Seidel and TDMA solver can be written as:

$$a_p T_p = a_w T_w + a_E T_E + b_p \longrightarrow (Gauss - Seidel)$$

Where $a_w = \frac{\lambda_w S_w}{d_{PW}}, a_E = \frac{\lambda_e S_e}{d_{PE}}, a_p = a_w + a_E$, $and\ b = q_v V_p$.

$$T[i] = P[i]T[i+1] + R[i] \longrightarrow (TDMA)$$

$where\ P[i] = \frac{a_e[i]}{a_P[i] - a_w[i]P[i-1]}\ and\ R[i] = \frac{b_P[i] + a_w[i]R[i-1]}{a_P[i] - a_w[i]P[i-1]}$

- First Node (i = 1)

To develop the equation of the first node, we will apply the energy balance at the boundary. As we know, at the boundary heat enters the boundary through convection and then it flows through cylinder as conduction. Therefore, the energy balance can be given as:

$$Q_{conv} = Q_{cond}$$

$$\alpha_A(T_A - T_p) = -\lambda_e \frac{T_e - T_p}{d_{PE}}$$

$$a_p T_p = a_w T_w + a_E T_E + b_p \longrightarrow (Guass\ Seidel)$$

Where $a_w = 0, a_E = \frac{\lambda_e}{d_{PE}}, a_p = a_E + \alpha_A$, $and\ b = q_v V_p$.

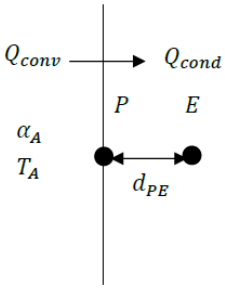

Fig. 5: First node

$$T[1] = P[1]T[2] + R[1] \longrightarrow (TDMA)$$

$where\ P[1] = \frac{a_E[1]}{a_P[1]}\ and\ R[1] = \frac{b_P[1]}{a_P[1]}$

- First Node (i = N+2)

Similarly, for node N+2 the same concept is applied to get the discretized equation, and it can be written as:

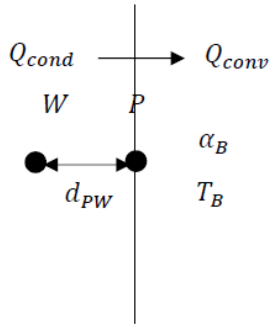

Fig. 6: Last node

$$Q_{cond} = Q_{conv}$$

$$-\lambda_w \frac{T_p - T_w}{d_{PW}} = \alpha_B (T_p - T_B)$$

$$a_p T_p = a_w T_w + a_E T_E + b_p \longrightarrow (Guass\ Seidel)$$

Where $a_w = \frac{\lambda_w}{d_{PW}}, a_E = 0, a_p = a_W + \alpha_B$, $and\ b = q_v V_p$.

$$T[N+2] = P[N+2]T[N+1] + R[N+2] \longrightarrow (TDMA)$$

$where\ P[N+2] = 0\ and\ R[N+2] = \frac{b_P[N+2] + a_W[N+2]R[N+1]}{a_P[N+2] - a_W[N+2]P[N+1]}$

CODE STRUCTURE

- Input Data

The first step is to provide input data, including physical and numerical parameters as outlined in Table 1.

- Mesh Definitions

Given the uniform meshing, the mesh size, control volume and node positions, areas and volumes are defined.

- Discretization Coefficients

The values discretization coefficients, $a_p, a_w, a_E\ and\ b_p$ are calculated for each node described above.

- Initialization of Temperature

The Initial temperature $T^*[i]$ was set to 0 at every node to start the code.

- Solution of Equations

For Guass-Seidel, the following equation is solved iteratively to calculate the new temperature of nodes from $i = 1\ to\ N+2$

$$a_p T_p = a_w T_w + a_E T_E + b_p$$

In case of TDMA, first the coefficients $P[i] and\ R[i]$ at each node are evaluated from $i = 1\ to\ N+2$. Then, the following equation is used iteratively to calculate the new temperature of nodes from $i = N+2\ to\ 1$

$$T[i] = P[i]T[i+1] + R[i]$$

- Stopping Criteria

There are two criteria to stop the loop: (1) firstly, the convergence criterion is used to check if the solution has reached the desired accuracy. The difference between new temperatures and previous temperatures ($T[i]$ - $T^*[i]$) is calculated. If it is less than desired accuracy, the temperature profile is saved, and we go to next of code. If not, new temperatures are assigned to $T^*[i]$ and new temperatures are calculated until desired accuracy is reached. (2) second criterion is of maximum iterations. If due to any reason, our solution does not converge, then code will run until maximum iterations are reached.

- Print the Results

Once the temperature profile with desired accuracy is obtained, it plotted to visualize the results.

CODE VERIFICATION

Following are the various methods that were used to verify the code.

- No heat generation and equal fluid temperatures

In this verification method, the temperatures of fluids on both sides were made equal, the thermal conductivity was kept constant, the heat generation was set to zero. Finally, the temperature profile was obtained as shown in Fig. 7. As expected, the temperature at each node) is equal to the fluids' temperature (constant temperature profile) because there is no heat transfer involved.

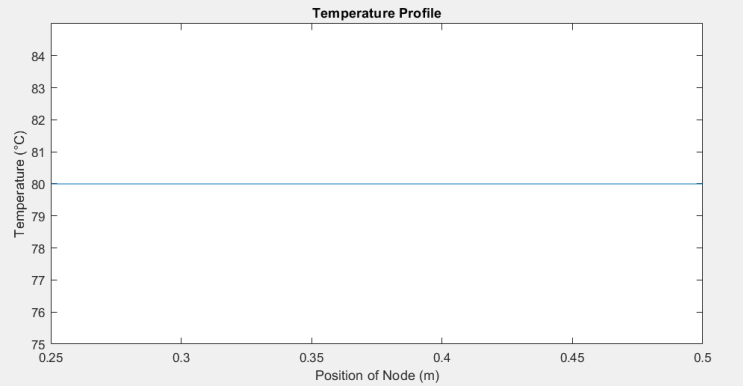

Fig. 7: Constant temperature profile

- Comparison with Analytical Solution

To compare with the analytical solution, the physical and numerical data were set to the values shown in Table 1. The temperature profiles using both analytical and numerical methods were obtained, and difference between temperatures at each node was calculated. It can be seen in Fig. 8 that the temperature profile from numerical method perfectly matches with that using analytical method with accuracy of 10^{-5}.

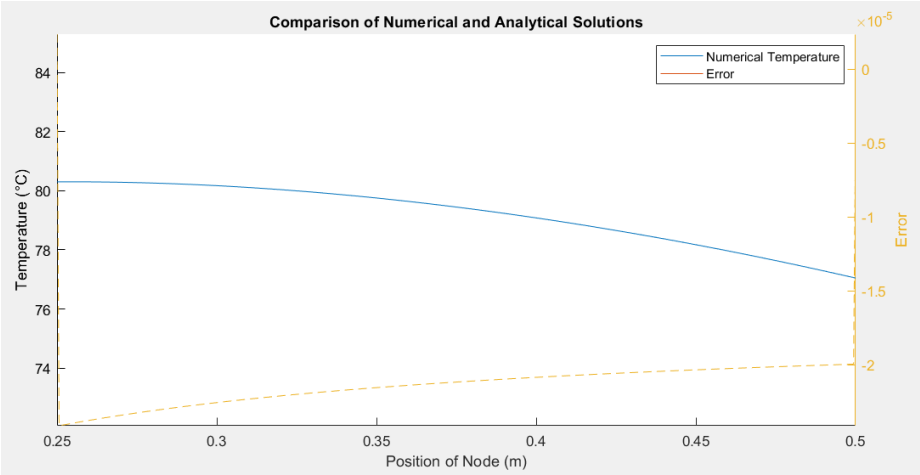

Fig. 8: Comparison with Analytical solution

- Global Energy Balance

The final verification method applied is to check the overall energy balance of the system. If the code is correct, the sum of heat fluxes and heat generation in the system must be equal to zero or equal to the desired order of accuracy.

$$Q_{boundary,in} + \sum q_{vi} V_{pi} - Q_{boundary,out} = 0 \; or \; equal \; to \; desired \; order \; of \; accuracy$$

The physical and numerical data was set to the values shown in Table 1, and the following results were obtained.

For Gauss-Seidel	**For TDMA**
$Q_{boundary,in} = -14.267743609727331\ W$	$Q_{boundary,in} = -14.267744386542724\ W$
$Q_{boundary,out} = 1163.829500131313\ W$	$Q_{boundary,out} = 1163.829500708246\ W$

$$\sum q_{vi}V_{pi} = 1178.097245096172\ W$$
$$Global\ Balance = 0.0000013551\ W = 1.3551e-6\ W$$

$$\sum q_{vi}V_{pi} = 1178.097245096172\ W$$
$$Global\ Balance = 0.0000000014\ W = 1.4e-9\ W$$

This is the desired accuracy. The error in global energy balance of Gauss-Seidel is higher than that of TDMA for same discretization coefficients. It is probably due to round off or solver residual error related to Gauss Seidel method.

MESH REFINEMENT STUDIES

- Impact of Number of Control Volumes

Fig. 9 shows the impact of number of control volumes (N) on the temperature profile of the cylinder obtained using numerical methods. Even the temperature profile is accurate for N = 10, however, as the number of control volumes increases, the temperature profile becomes more smooth and more accurate. Detailed impact is further shown in the following result.

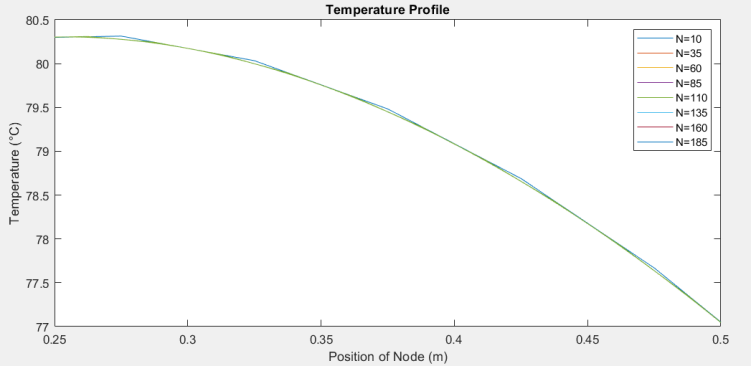

Fig. 9: Impact of number of control volumes

- Error Analysis

The impact of various mesh sizes was checked on the error (the difference between numerical and analytical solutions). As expected, as the mesh size decreases, the error between the numerical and analytical solutions also decreases. This can be attributed to the fact that with smaller mesh sizes we able to collect more data points therefore numerical solution tends to become more continuous and closer in nature to the analytical solution.

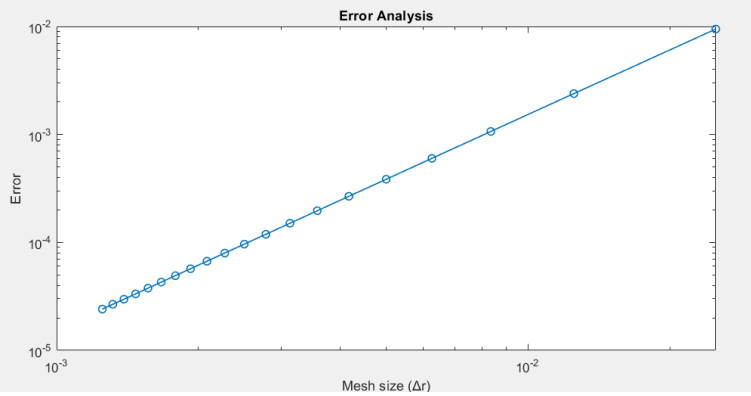

Fig. 10: Error analysis

RESULTS AND DISCUSSION

- Reference Case

Fig. 11 shows the temperature profile for the reference case. The values of the physical and numerical data for the reference case are shown in Table 1. Both the solvers provide the same solution, with temperature of internal boundary of around 80.3°C and it decreases as we go in outwards in radial direction with temperature of 77°C at external boundary.

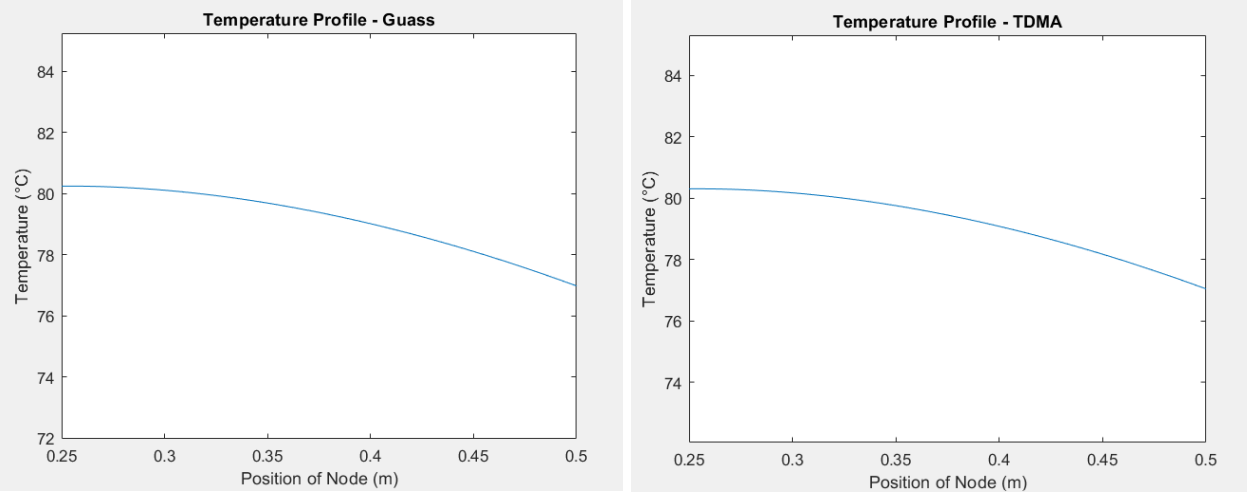

Fig. 11: Reference cases using Gauss-Seidel & TDMA

- Impact of Heat Generation

The steady state temperature profile was obtained for various values of heat generations with all the remaining physical and numerical data same as shown in Table 1. The value of heat generation was changed from 2000 to 3000 W/m^3, with an increment of 200 W/m^3. As anticipated, a higher heat generation rate results in an increased temperature throughout the cylinder. This is attributed to the limited thermal conductivity of the material, which restricts the rate of heat dissipation. Interestingly, the temperature gradient is steeper on the right wall of the cylinder compared to the left. This observation suggests that the heat loss from the right side of the cylinder is more significant due to the greater temperature difference between the external fluid and the cylinder surface at that location.

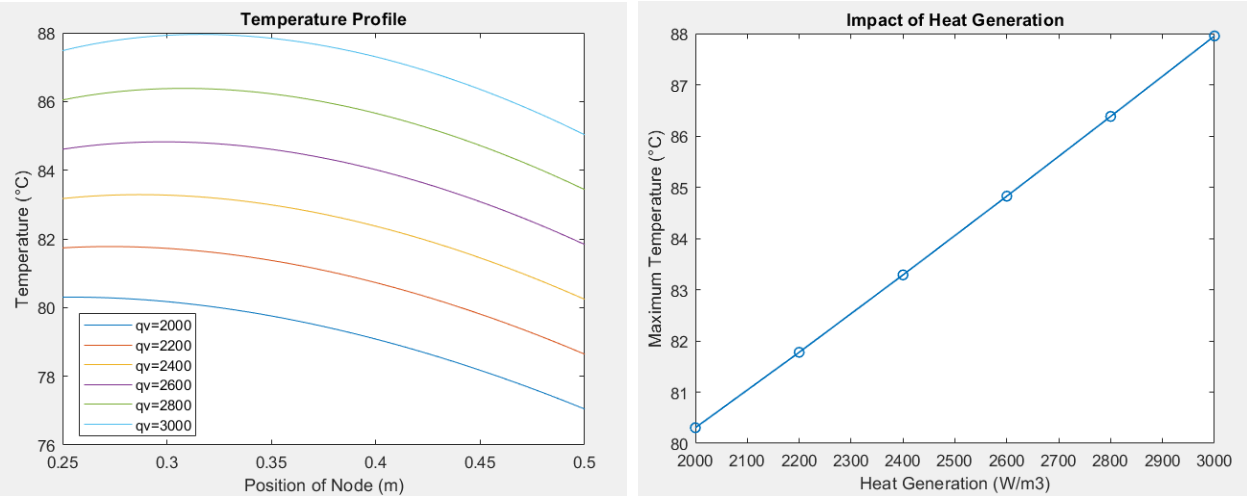

Fig. 12: Impact of heat generation

- Impact of Thermal Conductivity

Again, all the values of physical and numerical parameters except the thermal conductivity were kept constant. The thermal conductivity was changed from 15 W/m.K to 45 W/mK with an increment of 5 W/mK. As we can see, the higher the thermal conductivity results in lower temperatures for each node. This agrees with the physics of the problem because as thermal conductivity increases, heat spreads more effectively across the material, leading to a reduced temperature gradient and flatter profiles. Also, we observe all the temperature profiles pass through a single node, indicating that the temperature of that node remains constant. The intersection at a single node suggests that the temperature of this point is independent of λ, possibly due to a symmetry that keeps this temperature fixed regardless of the material's thermal conductivity.

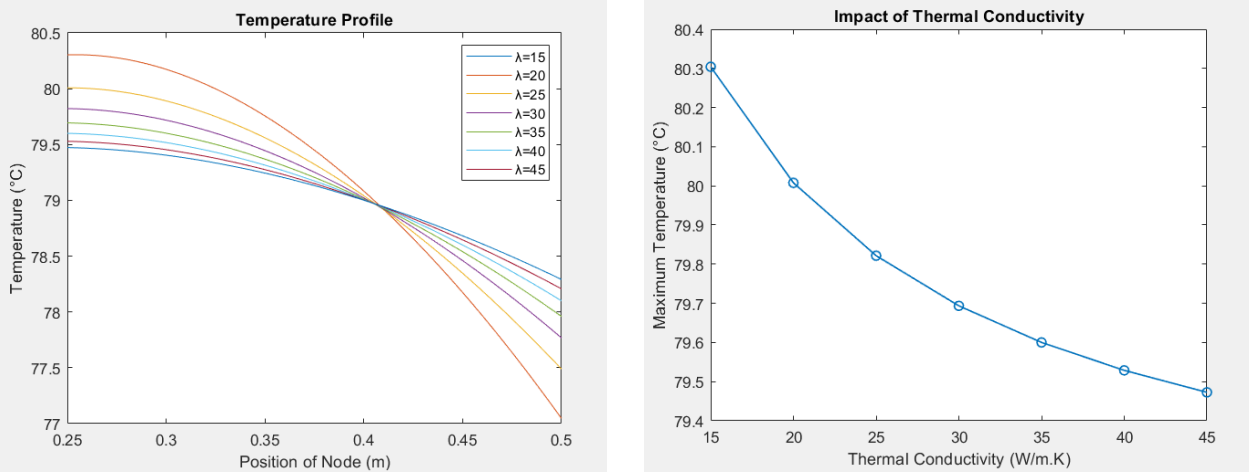

Fig. 13: Impact of thermal conductivity

- Impact of External Radius

Similarly, all the values of physical and numerical parameters except the external radius were kept constant. The external radius was changed from 0.5 to 1 m with an increment of 0.1 m. As observed, the increase in the value of external radius results in the increase in the temperature profile of the cylinder. This can be attributed to volumetric heat generation. Increasing the external radius means more volume which results in more volumetric heat generation with the same heat transfer coefficients. Also, a larger radius means a longer heat path to the boundary, causing heat to accumulate more in the central regions and resulting in higher peak temperatures. The temperature profiles show a greater gradient with smaller radius, while larger radius values result in flatter gradients, reflecting increased thermal resistance as the radius grows.

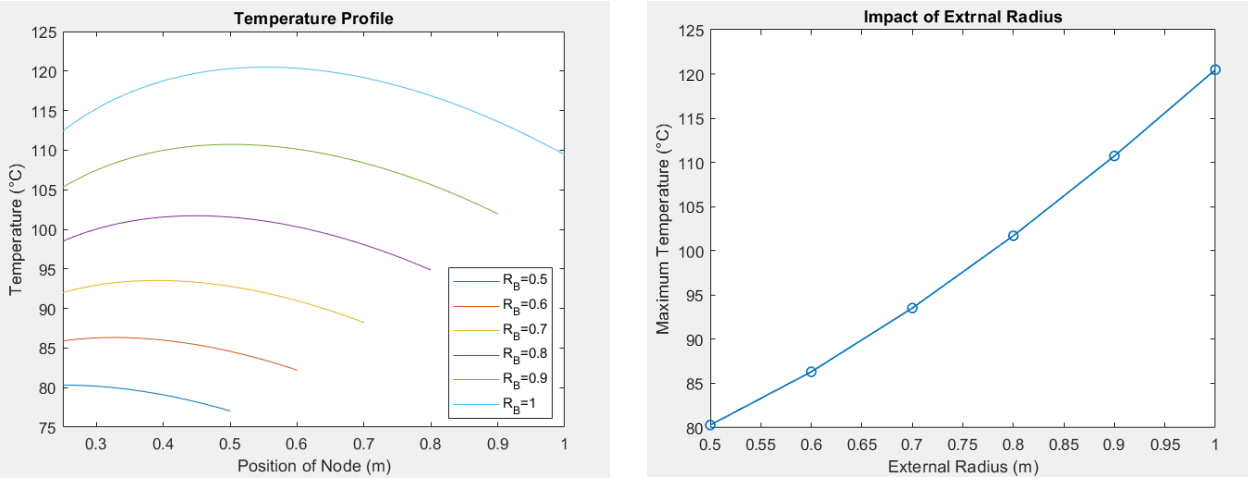

Fig. 14: Impact of External Radius